International Journal of Education and Science Research Review
E-ISSN 2348-6457
July- 2016, Volume-3, Issue-4
P-ISSN 2349-1817
www.ijesrr.org Email- editor@ijesrr.org

BIOLOGICAL STUDIES OF TANTALUM(V)- BARBITURIC ACID COMPLEX

DR. SHASHI LATA SINGH

Associate Professor, Department of Chemistry

R.R. College, Alwar, Rajasthan

Abstract

The perplexing age of M2+ particles (M = Ni and Cu) with L = barbituric acid (BA) in watery arrangement at °C and with an ionic strength of M (KNO3) in fluid medium has been read up for harmony. By ascertaining the ligand's separation constants, the basicity of the ligand was likewise evaluated. The BEST PC program was utilized to examine the trial pH titration information to decide the soundness constants of the various species delivered. The flow work shows the blend and careful portrayal of remarkable [Ta2(O2)6(carboxylate)2] peroxidotantalum(V) edifices connected to water solvent polymer (WSP) networks.- PAD (Ta(O2)3(sulfonate)2 and [PA = poly(sodium acrylate)] acid phosphatase (ACP) activities and their distinction as potent inhibitors.PSS [PSS = poly(4- Sodium Styrenesulfonate)] (PSSTa) Interestingly, using wheat thylakoid acid phosphatase as a model chemical, the peroxide tal (pTa) derivative was shown to be 2- to 3-fold more active as an ACP inhibitor (IC50 : 0.34 M for PSSTa), V-containing analogs (IC50: 1.22 M) using a series of tantalum (V) and vanadium (V) peroxides at equivalent full scales.

Keywords: *Biological, Tantalum(V), Barbituric, Acid, Phosphatase*

1. INTRODUCTION

The development of organ progress metal buildings with physiologically active ligands has received a ton of interest recently. The jobs of these ligands can be better perceived by research on such edifices in biological frameworks, which can likewise assist with the making of metal-based chemotherapeutics. Pyrimidine ring-containing substances are available in numerous vitamins, coenzymes, nucleic acids, and other biologically critical substances. They share similitudes with chemotherapeutic antimetabolites for treating disease in nucleic acids. Due to the large number of biological activities, including antimalarial, antibacterial, antitumoral, and antiviral activities, that pyrimidine metal edifices show, they have received expanded consideration lately. The

organometallic science of these ligands stood out, to a great extent from Beck and teammates in spite of the overflow of coordination edifices of pyrimidines.

Embed treatment has become broadly acknowledged in light of the fact that it provides biting execution that is equivalent to that of regular teeth and is the most favored choice in fixed substitution. It is fundamental for focus on the material component of dental inserts in innovative work because of the rising interest for embed treatment.

The subject of implantology has advanced incredibly since the invention of the principal dental embed useable shells around 600 Promotion. Dental inserts have generally been made of a variety of materials, including titanium, zirconia, and gold. The interest for the presentation of new materials and their improvisation has expanded alongside the consciousness of the acknowledgment of implantology as a technique for supplanting missing teeth.

In the domain of muscular health, tantalum has been utilized as an effective embed material. Tantalum is as of now receiving consideration as an expected material, notwithstanding the way that titanium right now is by all accounts a broadly acknowledged substance and is used in dental embed treatment. Its far and wide use and empowering results in muscular health have raised extraordinary familiarity with its expected use as a biocompatible embed material.

This might be made sense of by its promising qualities, including better bioactivity, decreased microbial attachment to the substrate, and the ability to produce apatite in reproduced organic liquid. Tantalum could sometime supplant titanium since it is the following nearest promptly open material and has more desirable characteristics than titanium. To improve osseointegration, various investigations and evaluations on titanium's surface change and treatment have been led before.

1.1. Context

Captivating structure blocks in the combination of natural mixtures incorporate barbituric acid 1, explicitly 2,4,6-(lH,3H,5H)- pyrimidinedione and its derivatives (Figure 1). When von Baeyer distributed a report on the creation of barbituric acid in 1894, this story initially started. Afterward, in 1903, Fisher and von Mering underscored the barbital's powerful mesmerizing characteristics as a pharmacological property of 5,5-diethyl barbituric acid, or "barbital". From that point forward, many complex models supportive in restorative science have been developed from barbituric acid derivatives, a field of study that has been the subject of various top to bottom reviews Figure 1 shows a couple of representative instances of the bioactive mixtures in this series and underscores the

significance of platforms with no less than one sound system genic focus or a tetrasubstituted carbon as wellsprings of compound variety and primary intricacy. The medication phenobarbital, used to treat a few types of epilepsy, is a derivative of barbital however has two unmistakable substituents at the C-5 position The development of several spiro-compounds and, thus, more inflexible structures was made conceivable by the twofold functionalization of barbituric acid's C-5 position These mixtures incorporate inhibitors of grid metalloproteinases (MMPs) and anticancer specialists . Then again, parts with one or the other antidiabetic or antituberculosis qualities were delivered by the blend of combined bike derivatives The photophysical properties of barbituric acid derivatives were utilized in colorimetric or heat discovery notwithstanding restorative science, and they likewise made promising colors or fluorogenic tests, to specify a couple.

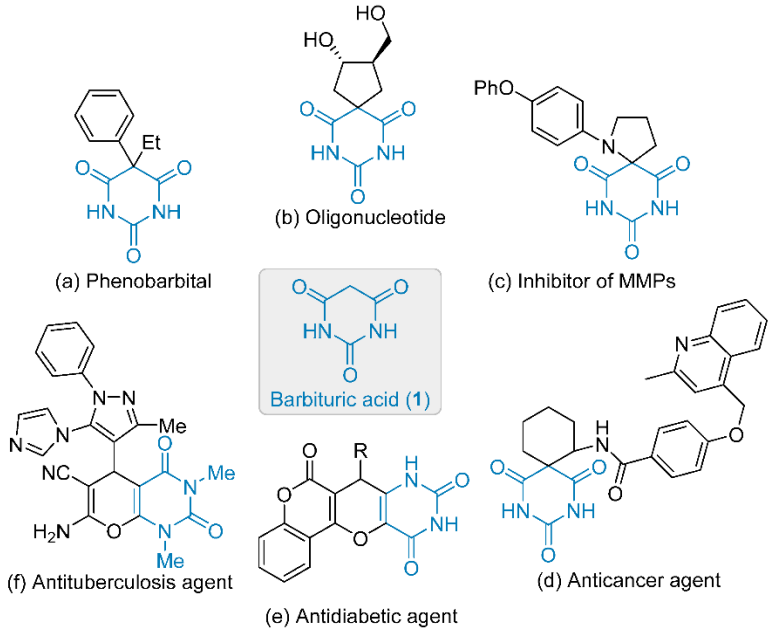

Figure 1: Barbituric acid platforms inside bioactive structures.

2. EXPERIMENTAL

2.1 Chemicals

Merck Compound Organization was utilized to acquire barbituric acid (BA). Aldrich Synthetic Organization and Merck Compound Organization provided the Ni(NO3)26H2O and Cu(NO3)23H2O, respectively. The reagents were all of scientific virtue and weren't additionally sanitized before use. The ultra water cleansing gear was utilized to acquire sans co2 twofold refined deionized water for the arrangements.

2.2 Titration Procedure

Ni(NO3)26H2O and Cu(NO3)23H2O were utilized to make arrangements of metal particles (0.01 M), which were then normalized utilizing ethylenediaminetetraacetic acid (EDTA) [21]. Using normalized NaOH, the convergence of the concentrated HCl was determined prior to making the HCl stock arrangement. The temperature was kept up with at °C by flowing water from a steady temperature shower during all potentiometric titrations on arrangements in a 100 mL twofold walled glass vessel utilizing a 10 mL needle, a Schott pH mix terminal, and the titroline programmed titration framework, which connection points to a PC. An attractive stirrer and a firmly fitting cover with three openings for the blend cathode, nitrogen gas, and programmed burette were incorporated with the cell. The environment of nitrogen was utilized to test the emf. The scope of ligand fixations was 2 103-6 103 M. Two significant cradles were normalized in the cell. The cradle arrangements had pH values of 4.0 and 7.0. By titrating a 0.01 M HCl arrangement with a sans carbonate 0,1 M NaOH arrangement at °C, the cathode was aligned on the log10 [H+] scale. The anode incline, figured utilizing the condition ()/(pH2 pH1), was inside >99% of the Nernstian value of 59.16 mV (pHunit)1. The hydrogen still up in the air from the emf values. At an ionic strength of 0.1 M, the of water was assessed to be 13.97.

The acid separation constants of the ligands were determined by potentiometric titration of the KNO 3 -modified ligand assembly (50 mL) with a constant ionic strength of 0.1 M (2×10 3 to 6×10 3 M). Es Found the constant. One titration accumulated 100 titration foci. All titrations were performed in a natural N2 environment using an aqueous titrant of 0.1 M NaOH.

There is no charge for straightness in the sense of a global stability constant.

$$\boldsymbol{P_M + qL + rH \leftrightharpoons [M_P\, L_q H_r]}$$

$$\boldsymbol{\beta_{pqr} = \frac{[M_P\, L_q H_r]}{[M]^p [L]^q [H]^r}}$$

3. RESULT AND DISCUSSION

Regardless of the way that the separation constants for barbituric acid have proactively been accounted for, we decided them involving potentiometric titration in the pH scope of 1.8 to 12.0 for our exploratory arrangement. Estimations were performed utilizing the BEST PC program. The got values and writing information are given in Table 1 for correlation. Given the variations in ionic strength, a fair concurrence with previously distributed results for BA is achieved. In watery arrangement, the BA divides into three species, H2L, HL, and L. Consider

$$H_2L \leftrightharpoons HL^- + H^+ \quad K_{a1} = \frac{[HL^-][H^+]}{[H_2L]}$$

$$HL^- \leftrightharpoons HL^- K_{a2} = \frac{[L^-][H^+]}{HL^-}$$

Table 1: Acid separation constants of Barbituric acid (BA) and the strength constants of the Ni(II), Cu(II)- BA buildings

Equilibrium	Constant	BA	Ni(II)	CU(II)
$H_2L \leftrightharpoons HL^- + H^+$	Log K_{h2L}	4.90±0.05 (4.82)		
$HL^- \leftrightharpoons L^{-2} + H^+$	Log K_{hL}	12.95±0.06 (13.40)		
PM+QL+rh$^-$⇋ $[M_pL_qh_R]$	Log β 110		7.75±0.10	9.40±0.06
	Log β 131		12.71±0.06	15.20±0.09
	Log β 140		18.99±0.06	20.21±0.06

3.1 Stability Constants of Ni(II)-BA Complexes

°C, Ni(II) in the ion array was subjected to potentiometric pH titration using 0.10 M KNO3 at a metal/ligand molar ratio of 1 1, 1: 2 and 1:3. For a metal/ligand molar ratio of 1:1, 12 and 1:

3, BA acid (strong) was added to the Ni(II) assembly. In Figure 1, a representative potentiometric titration curve for the Ni(II)-BA building is shown at 1 in addition to the titration curve for the free ligand (BA).1, 1:2 and 1:

Three stoichiometries are displayed. Examination of the complexed ligand curve (Figure 1) reveals the region of ligand that migrates into free ligand aggregates to lower pH due to swelling of the metal particles. This shows how reactions to complex products work by releasing protons from BA. 1 day:

he 1 Ni(II)-BA skeletal titration curve (curve 2 in Figure 1) shows two joint centers of = 1.0 and 2.2, and the base-to-metal ratio is expressed in molar units (Figure 1). Research has shown that no complications occur in the pH range of 6.0 to 11.0. The BA ligand acts as a bidentate chelating ligand because the imino N particle and one of its nearby carbonyl O ions are negatively charged.

Table 2: Potentiometric pH profiles for plans containing

ph	M
2.3	8
3.5	10
4.2	15
5.3	17
6.2	20
7.1	21
7.9	26

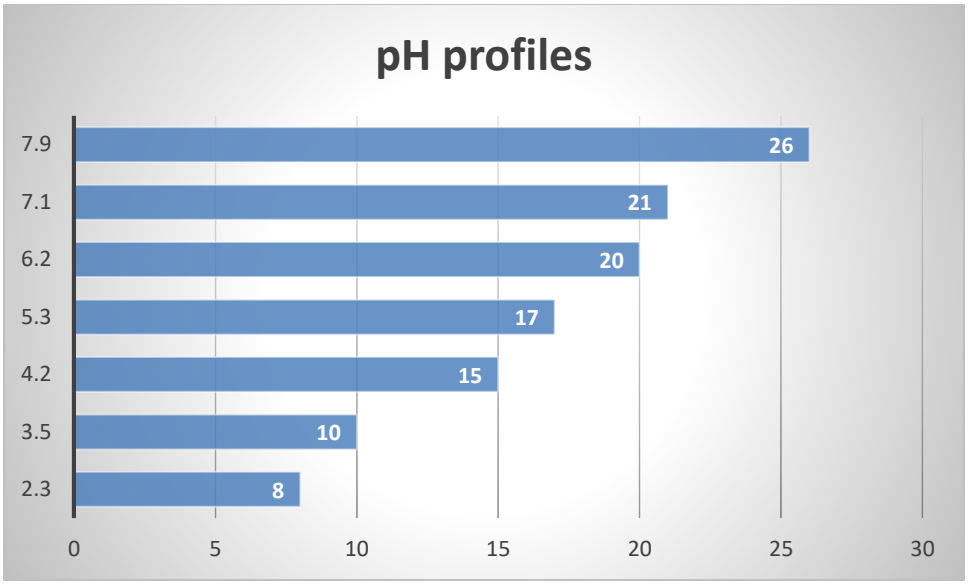

Figure 2: Potentiometric pH profiles for plans containing

The 1 : 2 Ni(II)- BA frameworks' potentiometric titrations were directed under the indistinguishable trial arrangement. Two expression focuses at 1.8 and 3.8 were tracked down in these curves. These protons' titrations in every one of these frameworks show that the development of the NiL2 complex is steady. The subsequent BA had similar ties as the main BA.

An indistinguishable experimental setup was used for the potentiometric titration of 1.

3 Ni(II)-BA framework. Titration of these protons in each of these scaffolds indicates slow construction of NiL3H complexes. However, it was only bound once to a third BA particle, either via a negatively charged iminonitor or carbonyl-O molecule. The building security constant is nothing, NiL2, and completely unset at 1.

Potentiometric titration at three mole fractions using the BEST PC program. Table 1 shows the safety constants for that building. For titration, the molar ratio of metal to ligand is 1:

Three propagation diagrams were created. These were acquired using SPE programming with the total focus of the metal particles set to 2 103 M. For framework BA and metallic particles Ni(II), the NiL3H species in Fig. 3 reaches a limit of 100 percent at pH 10.0. At a molar ratio of 1 mole of ligand to 1 mole of metal, the cutoff for the second species, NiL2, is 10% at pH 6.0, whereas the cutoff for the unpretentious species is 70%. .

3.2 Soundness Constants of Cu(II)- BA Edifices

Cu(II):Potentiometric titration of BA scaffolds was performed at °C in an ionic medium containing 0.10 M KNO3. The molar fraction of BA acid to Cu(II) aggregates was 1.1, 1:2 and 1:3. For the titration curve of 1:1 Cu(II)-BA framework (curve 2 in Figure 2) Two expression foci were observed at =1.0 and 2.2 (fraction of bases provided per mole of copper) (Figure 2). Furthermore, the titration curves for Cu(II) complexes are different from the free BA curves. According to experimental information, the CuL complex is formed at pH = 6.0–11.0 in the pH = 0–2.2 support zone.

Table 3: Potentiometric pH profiles of (I) BA-containing solutions

PH	m			
	I	II	III	IV
2	1.2	2.3	3.3	1.3
6	2.1	2.6	3.6	3.5
8	2.6	2.4	4.1	3.6
10	3.2	3.6	4.8	4.4
13	4.1	4.2	5.3	5.6

Figure 3: Potentiometric pH profiles of (I) BA-containing solutions

Table 4: As a function of pH, the metal ions Ni(II) and BA's species distribution curves for a solution initially comprising

PH	A(%)			
	Ni	NiL_2	NiL	NiL_3H
3	1.2	2.8	1.6	1.1
6	1.5	3.5	2.1	1.8
5	4.9	3.7	2.9	2.2
7	2.3	4.2	2.6	3.5
9	2.6	4.6	3.5	4.4
5	3.6	5.1	4.4	5.1

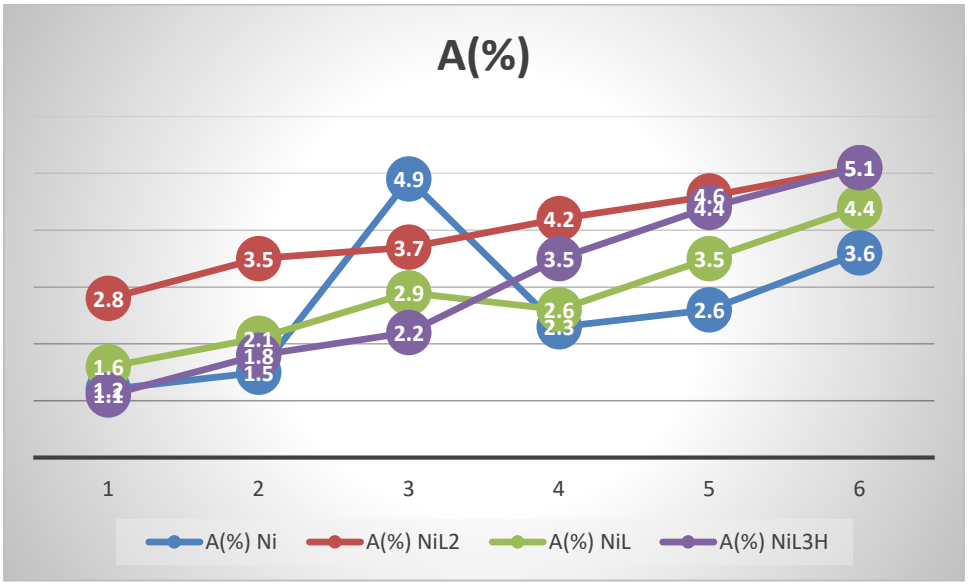

Figure 4: As a function of pH, the metal ions Ni(II) and BA's species distribution curves for a solution initially comprising

Under similar trial conditions, the 1 : 2 Cu(II)- BA frameworks' potentiometric titrations were performed. Two enunciation focuses in these curves were found at and. These protons' titrations in every one of these frameworks show that the development of the CuL2 complex is steady.

Under similar trial conditions, the 1 : 3 Cu(II)- BA frameworks' potentiometric titrations were performed. Two emphasis focuses in these curves were found at and. These protons' titrations in every one of these frameworks show that the arrangement of the CuL3H complex is slow. The BEST PC program was utilized to decide the soundness constants of the edifices CuL, CuL2, and CuL3H in the 1:3 molar proportion potentiometric titrations. Table 1 records the strength constants of their buildings.

For titration, the molar ratio of metal to ligand is 1:

3, got the spread map. These were obtained with the SPE program, with a total immobilized amount of metal particles of 2 × 103 M, set at 100%. For framework BA and metallic particle Cu(II), the CuL3H species in Fig. 4 reaches a threshold of 90% at pH 12.0. At pH 6.0–12.0, the second species, CuL2, reaches a cutoff of 60%, while the CuL complex species, with 1 mol of ligand available per mol of metal, has a 90% cutoff at pH 4.0–10. A cutoff of % is reached. .

Table 4: Distribution curves of Cu(II) and BA species as a function of pH of the initial containing solution

PH	A%			
	CU	CUL	CUL_2	CUL_3H
2	1.5	1.3	2.1	2.5
5	1.9	1.8	2.6	2.7
8	2.3	1.7	3.2	4.2
4	2.5	2.2	3.6	3.8
6	3.8	2.7	4.2	3.9
8	4.5	3.6	4.6	4.2

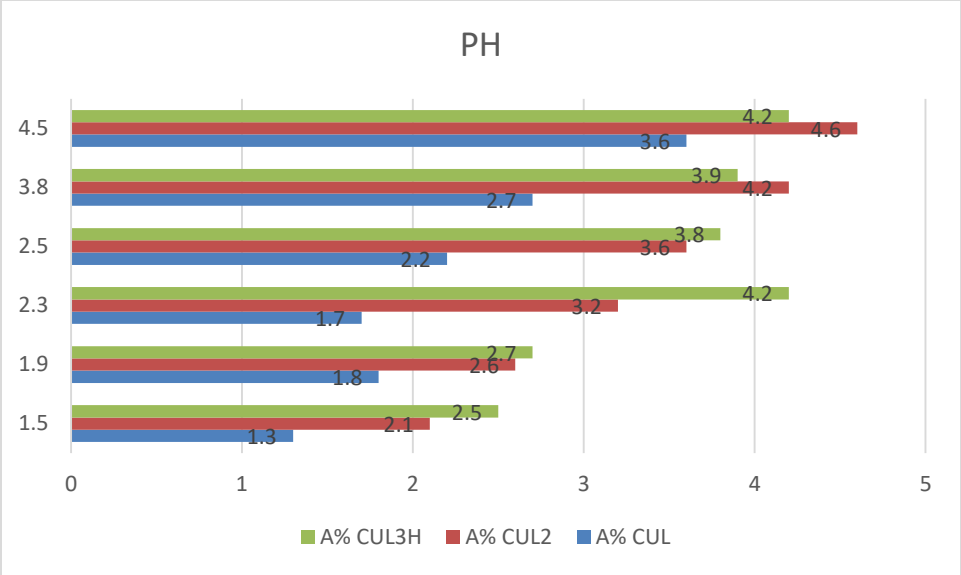

Figure 5: Distribution curves of Cu(II) and BA species as a function of pH of the initial containing solution

4. CONCLUSION

Enantioselective synergistic mixtures of chiral non-racemic barbiturates have raised interest in barbiturates as valuable building blocks for the development of both bio-related products and models with interesting properties relevant to materials science. Despite being established, it emerged gradually in the 1990s. The development of specific momentum or reactant strategies was critical to address the particular highlights of the undeniable Bronsted acidity of the barbiturates and the electrophilicity of the alkylidene equivalents. Isolation of sound systems with very equal utility for both nitrogen iota, even with non-linear barbiturate scaffolds, was difficult and required the use of creative strategic approaches. . However, barbituric derivatives can currently be used as impetuses for very enantioselective expansion and cycloaddition events to create novel chiral straight, combined, and spiro-bicyclic designs.

REFERENCES

1. *Baeyer, A. Mittheilungen aus dem organischen Laboratorium des Gewerbeinstitutes in Berlin: Untersuchungen über die Harnsäuregruppe. Justus Liebigs Ann. Chem. 1864, 130, 129–175.*
2. *Fischer, E.; von, M. New class of narcotics. Ther. Ggw. 1903, 44, 97–101.*
3. *Moussier, N.; Bruche, L.; Viani, F.; Zanda, M. Fluorinated Barbituric Acid Derivatives: Synthesis and Bio-activity. Curr. Org. Chem. 2003, 7, 1071–1080.*

4. *Bojarski, J.T.; Mokrosz, J.L.; Barton, H.J.; Paluchowska, M.H. Recent progress in barbituric acid chemistry. Adv. Heterocycl. Chem. 1985, 38, 229–297.*
5. *Sans, R.G.; Chozas, M.G. Historical aspects and applications of barbituric acid derivatives. A review. Pharmazie 1988, 43, 827–829.*
6. *Nikoofar, K.; Khademi, Z. Barbituric Acids in Organic Transformations, An Outlook to the Reaction Media. Mini-Rev. Org. Chem. 2017, 14, 143–173.*
7. *Bialer, M. How did phenobarbital's chemical structure affect the development of subsequent antiepileptic drugs (AEDs)? Epilepsia 2012, 53, 3–11.*
8. *Renard, A.; Lhomme, J.; Kotera, M. Synthesis and Properties of Spiro Nucleosides Containing the Barbituric Acid Moiety. J. Org. Chem. 2002, 67, 1302–1307.*
9. *Kim, S.-H.; Pudzianowski, A.T.; Leavitt, K.J.; Barbosa, J.; McDonnell, P.A.; Metzler, W.J.; Rankin, B.M.; Liu, R.; Vaccaro, W.; Pitts, W. Structure-based design of potent and selective inhibitors of collagenase-3 (MMP-13). Bioorg. Med. Chem. Lett. 2005, 15, 1101–1106.*
10. *Fessenden, R.J.; Larsen, J.G.; Coon, M.D.; Fessenden, J.S. Silicon Heterocyclic Compounds. III. Silicon-Substituted Spirobarbiturates. J. Med. Chem. 1964, 7, 695–698.*
11. *Duan, J.J.W.; Chen, L.; Lu, Z.; Jiang, B.; Asakawa, N.; Sheppeck, J.E.; Liu, R.-Q.; Covington, M.B.; Pitts, W.; Kim, S.-H.; et al. Discovery of low nanomolar non-hydroxamate inhibitors of tumor necrosis factor-α converting enzyme (TACE). Bioorg. Med. Chem. Lett. 2007, 17, 266–271.*
12. *Ingle, V.N.; Gaidhane, P.K.; Dutta, S.S.; Naha, P.P.; Sengupta, M.S. Synthesis of Novel Galactopyranosyl-Derived Spiro Barbiturates. J. Carbohydr. Chem. 2006, 25, 661–671.*
13. *Hese, S.V.; Meshram, R.J.; Kamble, R.D.; Mogle, P.P.; Patil, K.K.; Kamble, S.S. Antidiabetic and allied biochemical roles of new chromeno-pyrano pyrimidine compounds: Synthesis, in vitro and in silico analysis. Med. Chem. Res. 2017, 26, 805–818.*
14. *Kalaria, P.N.; Satasia, S.P.; Raval, D.K. Synthesis, characterization and biological screening of novel 5-imidazopyrazole incorporated fused pyran motifs under microwave irradiation. New J. Chem. 2014, 38, 1512–1521.*
15. *Gomes, R.F.A.; Coelho, J.A.S.; Afonso, C.A.M. Synthesis and Applications of Stenhouse Salts and Derivatives. Chem. Eur. J. 2018, 24, 9170–9186.*